Using UWB IR Radar Technology to Decode Multiple Chipless RFID Tags

Marvin Barahona, Diego Betancourt and Frank Ellinger
Chair for Circuit Design and Network Theory
Technische Universität Dresden
Dresden, Germany

***Abstract*—In this paper, a technique to decode multiple ultra-wide band (UWB) chipless radio frequency identification (RFID) tags using UWB impulse radio (IR) radar technology is proposed. The methodology presented is proven for decoding several chipless RFID tags simultaneously placed in the reader's identification zone, and it is based on the analysis of the received pulses backscattered from chipless tags located at the same or different distance from the radar. The decoding takes places using an algorithm that analyzes the backscattered pulses time-difference-of-arrival (TDOA), energy and the chipless tags coding to detect tags-collision scenarios. Several chipless tags having either the same or different code within the UWB frequency range from 4 to 8 GHz are fabricated using aluminum on polyethylene terephthalate (PET) substrate. The technique is validated experimentally using the UWB IR radar principle and technology to perform the decoding of multiple chipless RFID tags simultaneously placed in reader's identification zone. The chipless RFID tags are successfully decoded in eight different combinations scenarios.**

Keywords— ultra-wide band, UWB, UWB chipless RFID Tag, RFID, Radar Cross Section, RCS, Decoding

I. INTRODUCTION

The UWB chipless RFID systems being investigated today are trying to include more features to a comparative tag price to the ones being offered by the barcode technology. Barcodes are scanned one at the time and their scanners might require to be maneuvered to the correct position between successive reads, limiting the read rate of the whole process [1]. On the other hand, with the conventional and chipless RFID technologies, several tags could be read automatically by placing the different tagged items in a convey belt and then detect them as they pass through the identification zone, significantly reducing the reading process time without the need of human intervention. Furthermore, the possibility to detect multiple tags simultaneously placed in the reader's identification zone is one of the key capabilities these RFID systems should offer, providing another unique advantage to speed up further these processes, especially in applications like logistics and supply chain management.

Another application being investigated for the use of the chipless RFID technology is its implementation for evacuations procedures [2]. As shown in Fig. 1, when several persons are being evacuated from a dangerous situation, the UWB chipless RFID system should be able to assess the type and correspondent amount of codes of the UWB chipless RFID tags attached to the tickets they hold in their hands. Then, the decoded information is matched with the correspondent code interpretation (e.g. 2 adults). Nevertheless, when several chipless tags are located simultaneously in the reader's identification zone and respond to the same interrogation signal, a tag to tag collision occurs [3]. The chipless tags are memoryless and can't be programmed with algorithms to help the reader to avoid collisions like in the conventional RFID tags (i.e. with chips) case [4], [5], [6]. Therefore, a major challenge lies in how the UWB chipless RFID system should achieve this goal.

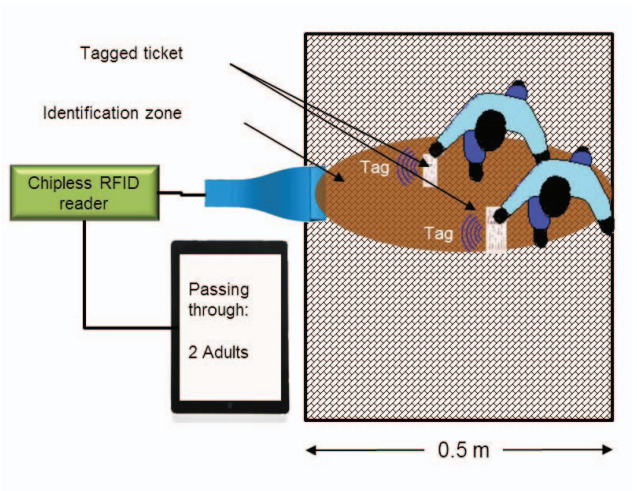

Fig. 1: Decoding of multiple chipless tags, modified from [11].

The chipless RFID tags are usually fabricated using metallic resonators, which produce a unique radio frequency (RF) signature for each code. Adding extra resonance frequencies to implement any type of anti-collision protocol in chipless tags, simply translates in a change in the chipless tag's overall code when seen from the used spectrum perspective, and it could finally mean that many different codes are generated to identify just one type of item in a multiple tag scenario. On the other hand, if the decoding is to be conducted without implementing any anti-collision protocol at the chipless tags, the chipless tag coding itself should provide enough robustness to help to overcome or detect the collision,

The research leading to these results received funding from the European Union's Seventh Framework Program (FP7/2007-2013) under grant agreement No. 313161; eVACUATE Project (further info available at www.evacuate.eu)

978-1-5090-1317-3/16/$31.00 ©2016 IEEE

and the reader should increase its complexity and processing load to be able to perform the collision detection and successfully decode the type and amount of chipless tags. In [7] and [8] a short-time matrix pencil method (STMPM) is implemented to decode multiple chipless RFID tags for different reader's configurations. In [9] a linear frequency modulated signal is used as an interrogation signal (LFM) and fractional Fourier transform (FrFT) is employed to separate the responses from multiple tags and in [10] a collision detection method based on frequency-modulated continuous-wave (FMCW) radar is proposed.

This paper presents a line-of-sight (LOS) and multipath free decoding technique for multiple chipless tags simultaneously placed in the reader's identification area. The collision detection is implemented at the reader and based on three different approaches, TDOA for the case when the chipless tags are placed at different distances. For the case when the tags are placed next to each other, backscattered pulse-energy-modulation (B-PEM) is used to decode same coded-tags based in [11]. And for different coded-tags, a frequency shift based tag coding robust enough to be able to decode them using a correlator is implemented. The decoding is performed in the time domain, correlating the received backscattered pulses to the previously stored chipless tags codes templates. The chipless tags are fabricated and measured under normal conditions with a commercial IR-radar and a range distance of 50 cm in one of the offices at the Technische Univeristät Dresden.

II. Tags Fabrication and Test Procedures

A. Tags design and coding

The tags used for this investigation are a modified version of the ones described in [12], given that these tags have been designed to work in the same working frequency range from 4 to 8 GHz as the commercial UWB IR radar. Fig. 2(a) shows the chipless tags A and B shapes, and Fig. 2(b) their simulated radar cross section's magnitude |RCS| using CST Microwave Studio. The tags coding also differs from to the ones in [12], where silver ink drops are used to short circuit the resonators and the coding is performed by the presence or absence of dips. Here, the codification used for these two tags is the dip's frequency shift generated by changing the dimensions of the resonators width, as can be seen in Fig. 2. Additionally, the frequency shift coding is chosen in a way that the correlation values between different codes are different enough to guarantee its successful detection. Furthermore, the combination of the two codes (i.e. A + B) generates a third frequency response which is also different from the first two codes which generated it, as shown in Fig. 2(b). This difference allows that the generated frequency response of the combined chipless tags is processed as an extra tag code. Finally, the chipless tags are fabricated using aluminum tape and PET, following the procedure described in [13].

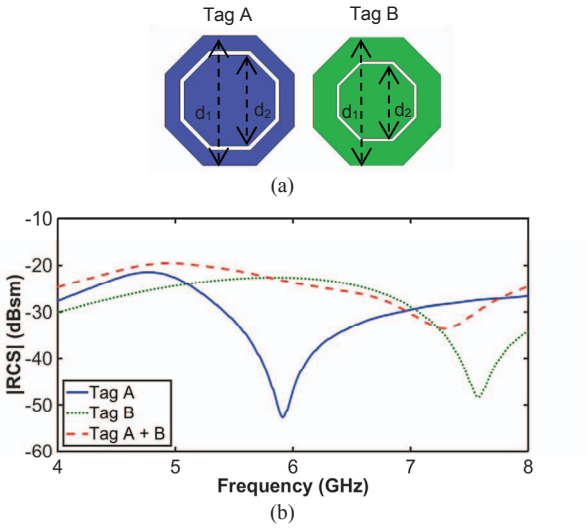

Fig. 2: (a) Chipless tags designs, tag A: d_1 = 22.4 mm, d_2 = 15.3 mm, resonator thickness of 2.7 mm, tag B: d_1 = 22.4 mm, d_2 = 12.4 mm and resonator thickness = 4.45 mm. (b) Simulated chipless tags |RCS| response.

B. Detection scenarios and test procedures

The line-of-sight and multipath free scenarios for the simultaneous decoding of the two chipless tags are depicted in Fig. 3. Given the IR radar's range resolution limitations, all scenarios consist of different sets of chipless tags, located at distances of 10 or 30 cm from the antennas, in order to guarantee enough time delay between each received pulse and clearly distinguish between them. A direct line-of-sight to the tags is required to be able to backscatter the signal pulse directly back to the antennas. The influence of multipath components is avoided by placing the antennas at a height of 80 cm, which is eight times the direct distance between the antennas and the tag located at the closest position. Additionally, the distances from the antennas to the rest of the surrounding surfaces are in the order of several meters.

The measurements of the backscattered pulses of each UWB chipless tags scenario are performed using the radar test set up shown in Fig. 4 and for the VNA measurements the one described in [13], mounted under normal circumstances in one of the offices at the Technische Universität Dresden. The radar based test set up consists of two vertically polarized horn antennas (Chengdu AINFO Inc. LB-OH-159-10-C-SF) separated 10 cm from each other and capable to operate in the frequency range from 4 to 8 GHz with a variable linear gain from 7 dBi at 4 GHz to 14 dBi at 8 GHz. The Novelda radar connected to the antennas measures and sends the backscattered time response of the chipless tags to a personal computer with the Matlab® script to perform the detection. One scan per measurement scenario is sent by the radar to perform the tags set readings.

The UWB chipless RFID tags are mounted on different tripods and placed with direct line-of-sight at distances of either 10 or 30 cm from the horn antennas, as shown in Fig. 4. One reference measurement of the backscattered pulse of every single tag A, B and their generated code A + B placed at each distance is required to further serve as a comparison template signal in the decoding stage. The different scenarios configurations shown in Fig. 3 are set and also measured. The frequency domain analysis is performed with the calibration technique described in [14] for the one tag measurements case. For the set of two or more tags case, the no tag and reference measurements are performed removing only the tag of the position where the measurement should take place and leaving the other tag at its location. The measurements are done in the

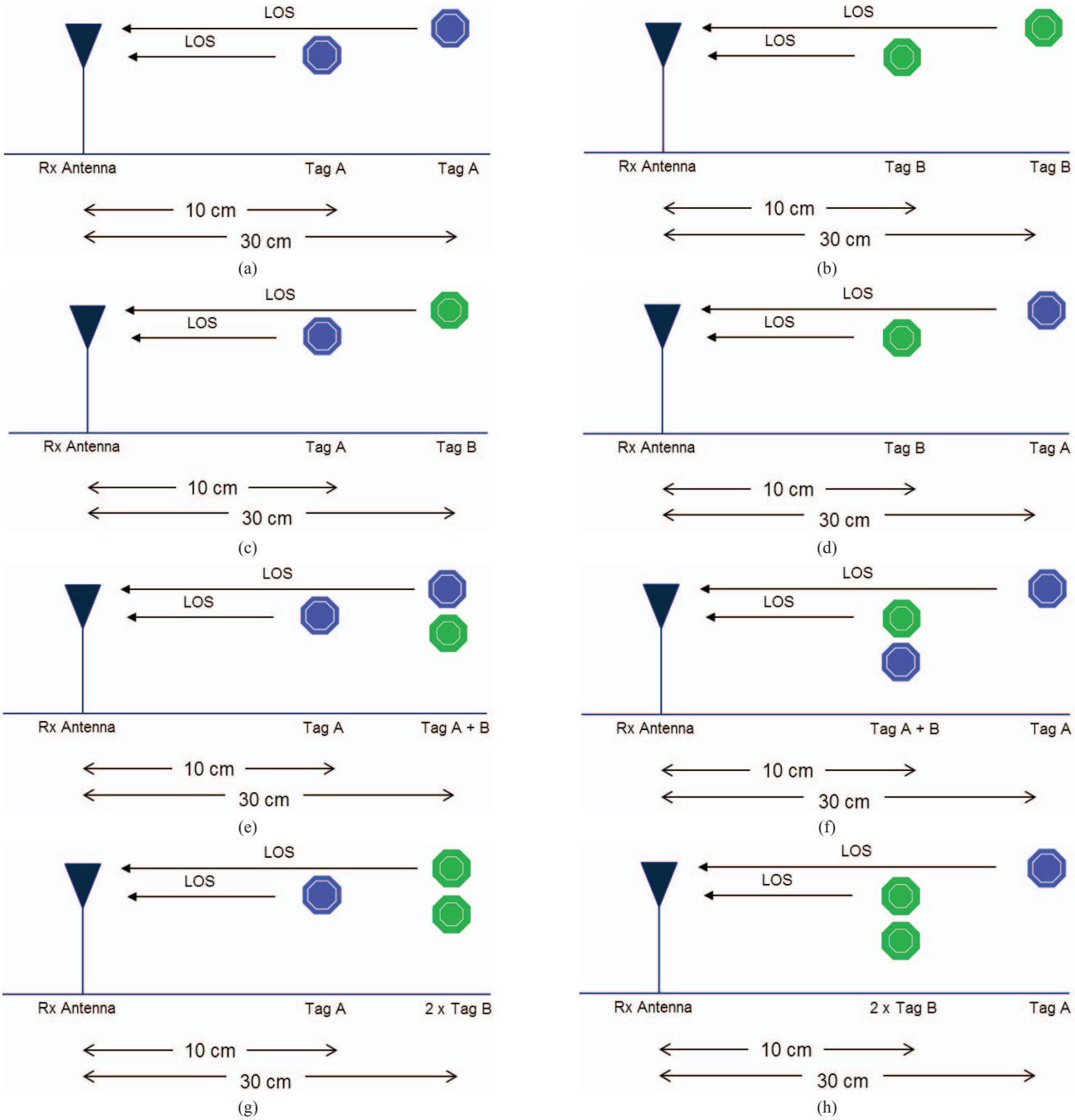

Fig. 3: Multiple chipless tags simultaneous line-of-sight detection scenarios: (a) A – A, two type A tags located at 10 and 30 cm from the antennas, (b) B – B, two type B tags located at 10 and 30 cm from the antennas, (c) A – B, tag A located at 10 cm and tag B at 30 cm from the antennas, (d) B – A, tag B located at 10 cm and tag A at the 30 cm from the antennas, (e) A – A + B, tag A located at 10 cm and tags A + B at 30 cm from the antennas (f) A + B – B, tags A + B located at 10 cm and tag B at 30 cm from the antennas, (g) A – 2B, tag A located at 10 cm and 2 tags B at 30 cm from the antennas, and (h) 2B – A, 2 tags B located at 10 cm and tag A at 30 cm from the antennas.

time domain and therefore the Fast Fourier transform (FFT) is used to obtain its frequency domain values.

To perform the decoding, the pulses $p_{A,B,A+B}$ corresponding to the single measurement of the chipless tags A, B or A + B are normalized according to equation (1) [15], to make the signals comparable. The received two pulses $p_{1,2}$ of the different tag detection scenarios are processed individually and also normalized according to equation (1) as previously done for the single tag case. The next step involves performing the correlation $r_{p_m p_t}$ between each scenario's received pulse $p_{1,2}$ and the two previously stored single tag pulses $p_{A,B,A+B}$ at the respective distance, following the equation (2) [16]. The correlation to the stored signal with the highest value is the one considered as the tag or tags being present in the analyzed pulse.

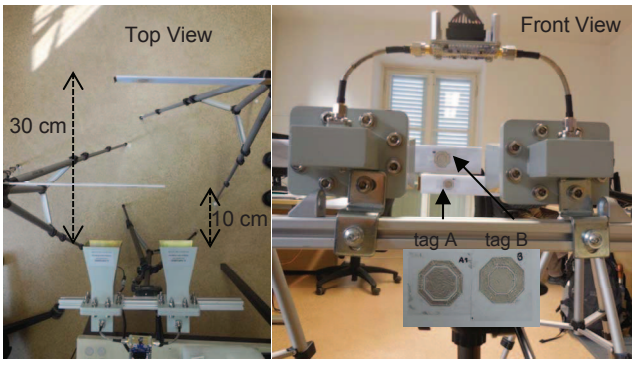

Fig. 4: Picture of the radar based test setup used to detect the UWB chipless RFID tags. The tags are placed with direct line-of-sight at distances of 10 and 30 cm to the horn antennas.

$$p_q(n) = \frac{p_q(n) - \mu_q}{\sigma_q} \quad (1)$$

$q = A, B, A + B, 1, 2$

μ: pulse's mean

σ: pulse's standard deviation

$$r_{p_m p_t}(l) = \sum_{n=-\infty}^{+\infty} p_t(n) p_m(n - l) \quad (2)$$

$l = 0, \pm 1, \pm 2, \ldots$

$m = 1, 2$

$t = A, B, A + B$

Finally, once the tag decoding has taken place, the amount of same-code tags is estimated using the received energy values $\varepsilon_{A,B}$ calculated using equation (3) [16].

$$\varepsilon_t = \sum_{-\infty}^{+\infty} |p_t(n)|^2 \quad (3)$$

III. Measurement Results

The experimental validation is performed following the procedure described in the previous section. The results of the frequency domain analysis are shown in Fig. 5, as can be seen, all measurements follow the same shape for the specific analyzed tag and also to its simulated values in Fig 2(b). Frequency shifts of up to 200 MHz between measurements at different distances can be observed, which are mainly caused by the signal shape inaccuracies of the Novelda's commercial UWB IR radar setup. Unlike the radar technology, where only the pulse delay is mostly analyzed to determinate the target's distance, in chipless RFID applications the pulse's shape is important to be able to successfully decode the tag.

The obtained correlation results are shown in Fig. 6, as can be seen in all graphs, despite the variations observed in the frequency domain, the correlation values clearly identifies the correct tag from where the pulse is backscattered at each specific scenario. Furthermore, the calculations were also performed using only one reference pulse per tag type at either

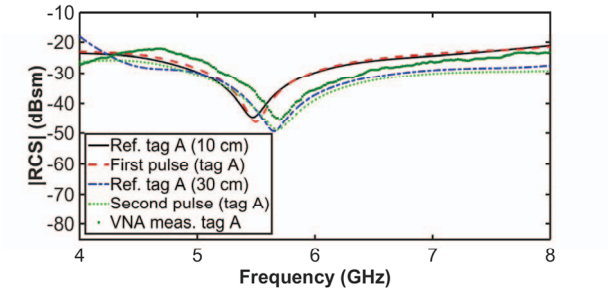

(a)

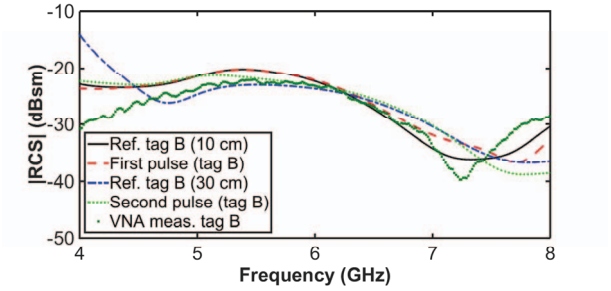

(b)

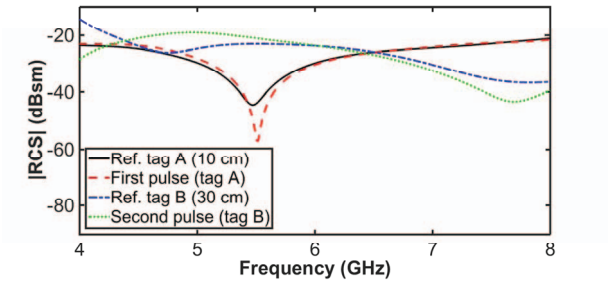

(c)

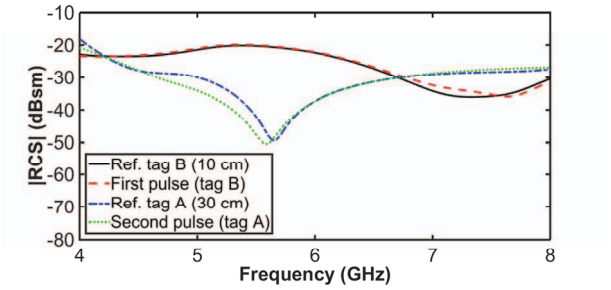

(d)

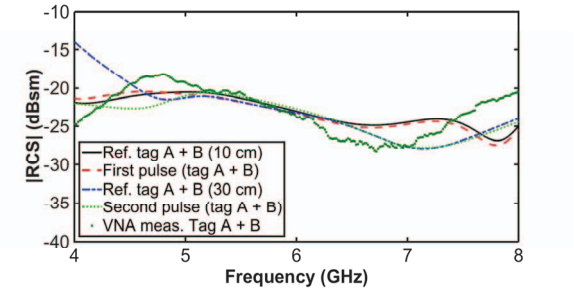

(e)

Fig. 5: Calculated frequency response of stored single tags and detection scenarios. (a) A – A and VNA measurements of tag A, (b) B – B and VNA measurements of tag B, (c) A – B, (d) B – A , and (e) only A + B responses of scenarios A – A + B, A + B – A and VNA measurement of A + B.

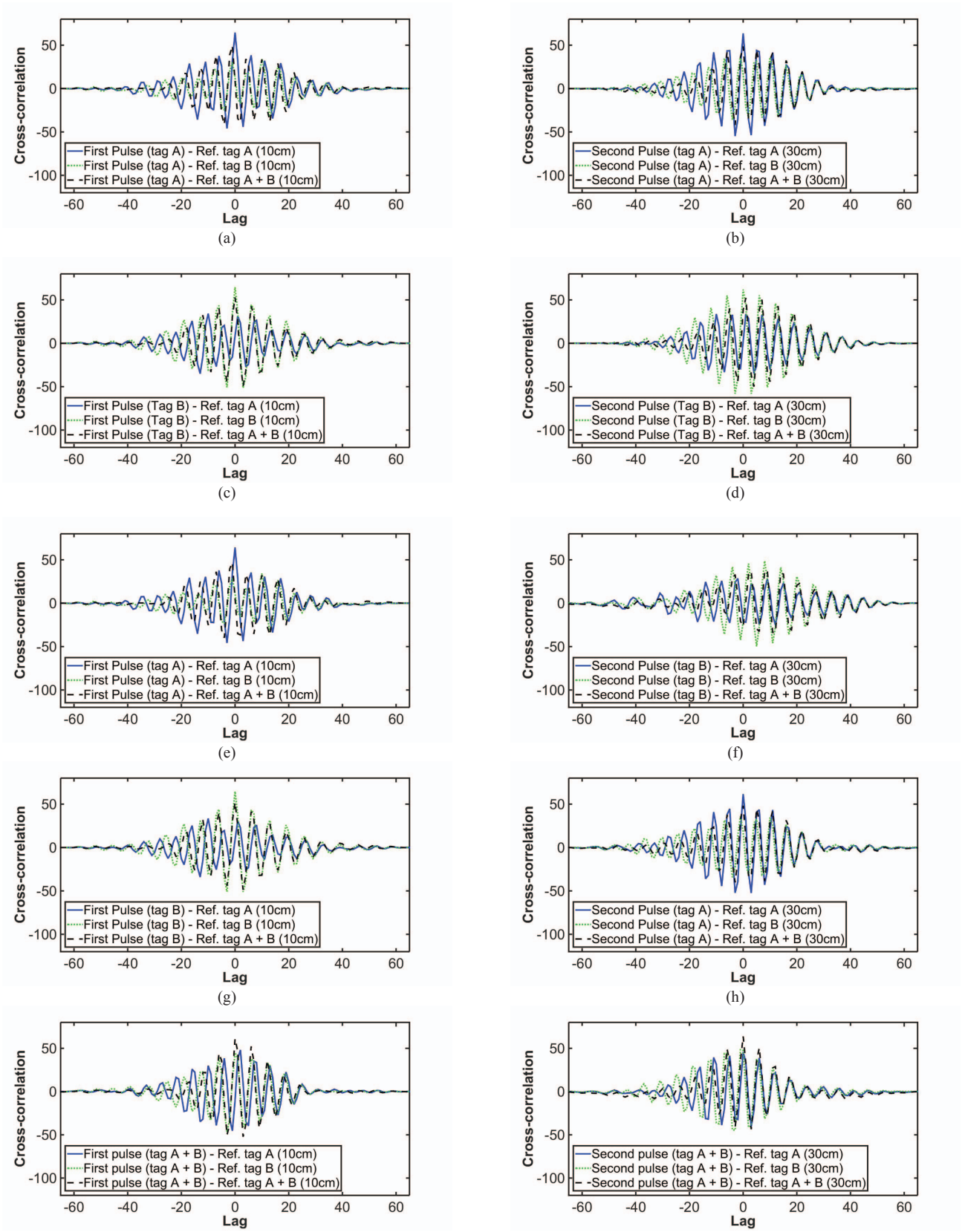

Fig. 6: Correlation of: (a) first pulse of scenario A – A with reference pulses of tags A, B, and A + B located at 10 cm, (b) second pulse of scenario A – A with reference pulses of tags A, B, and A + B located at 30 cm, (c) first pulse of scenario B – B with reference pulses of tags A, B, and A + B located at 10 cm, (d) second pulse of scenario B – B with reference pulses of tags A, B, and A + B located at 30 cm, (e) first pulse of scenario A – B with reference pulses of tags A, B, and A + B located at 10 cm, (f) second pulse of scenario A – B with reference pulses of tags A, B, and A + B located at 30 cm, (g) first pulse of scenario B – A with reference pulses of tags A, B, and A + B located at 10 cm, (h) second pulse of scenario A – B with reference pulses of tags A, B, and A + B located at 30 cm, (i) first pulse of scenario A + B – A with reference pulses of tags A, B, and A + B located at 10 cm,, and (j) second pulse of scenario A – A + B with reference pulses of tags A, B, and A + B located at 30 cm.

10 or 30 cm and the decoding were still successful.

The received pulse energy calculations including the path loss are shown in Table I, the values shows a clear different between the amounts of chipless tags are placed together to the case when only one tag is present. Therefore, by setting the proper energy thresholds, the right amount of tags can be assessed.

TABLE I. PULSE ENERGY CALCULATIONS

Received pulse energy (μJ)			
Amount	***Type of tag***	***10 cm***	***30 cm***
1	Tag A	0.81	0.69
2	Tag A	2.59	2.01
1	Tag B	1.50	1.44
2	Tag B	3.61	2.82

IV. CONCLUSIONS

This paper has presented a line-of-sight UWB IR radar technique to simultaneously decode chipless tags. The experiment is conducted using frequency shift coded chipless tags fabricated with aluminum tape on PET and commercial UWB IR radar.

Chipless tags are successfully decoded when simultaneously placed in the reader's identification zone for different line-of-sight scenarios. The received backscattered pulses delayed in time are analyzed individually, correlated to their previously single/combined tag stored references and finally the amount of same-coded tags placed at the same distance is determinate by the pulse energy calculations.

REFERENCES

[1] L. Bolotnyy and G. Robins, "The case for multi-tag RFID systems," in *Proc. International Conference on Wireless Algorithms, Systems and Applications (WASA),* Aug. 1 – 3, 2007, pp. 174 – 186.

[2] D. Betancourt et al., "Square-shape fully printed chipless RFID tag and its applications in evacuation procedures," in *Proc. 9th European Conf. on Antennas and Propagaton (EuCAP)*, May 13 – 17, 2015, pp. 1 – 5. C.

[3] C. Meguerditchian, H. Safa, and W. El-Hajj, "New reader anti-collision algorithm for dense RFID enviroments," in *Proc. IEEE international Conference on Electronics, Circuits and Systems (ICECS),* Dec. 11 –14 , 2011, pp. 85 – 88.

[4] W. Su , N. Alchazidis, and T. Ha, "Multiple RFID tags access algorithm," *IEEE Transactions on Mobile Computing*, Vol. 9, Jun. 2009, pp- 174 – 187.

[5] C. Galiotto et al., "High fairness reader anti-collision protocol in passive RFID systems," in *Proc. IEEE International Conference on RFID (IEEE RFID)*, Apr. 12 – 14, 2011, pp. 113 – 120.

[6] D. Shen, G. Woo, D. Reed, A. Lippman, and J. Wang, "Separation of multiple passive RFID signals using software defined radio," in *Proc. IEEE International Conference on RFID (IEEE RFID)*, Apr. 28 – 29, 2009, pp. 139 – 146.

[7] M. Rezaiesarlak, and M. Manteghi, "A spacetimefrequency anticollision algorithm for identifying chipless rfid tags," *IEEE Transactions on Antennas and Propagation*, Vol. 62, No. 3, pp. 1425 – 1432, Mar. 2014.

[8] R. Rezaiesarlak and M. Manteghi, "A new anti-collision algorithm for identifying chipless rfid tags," in *Proc. IEEE Antennas and Propagation Society International Symposium (APSURSI)*, Jul. 7 – 13, 2013, pp. 1722– 1723.

[9] R. Azim and N. Karmakar, "A collision avoidance methodology for chipless tags," in *Proc. Asia-Pacific Microwave Conference (APMC)*, Dec. 5 – 8, 2011, pp. 1514–1517.

[10] R. Azim, and N. Karmakar, "Efficient collision detection method in chipless RFID systems," in *Proc. International Conference on Electrical & Computer Engineering (ICECE),* Dec. 20 – 22, 2012, pp. 830 – 833.

[11] M. Barahona, D. Betancourt, and F. Ellinger, "Decoding of nultiple same-coded in-line placed chipless RFID tags," in *Proc. IEEE Conference on Antenna Measurements & Applications (CAMA),* Nov. 16 - 19, 2014, pp. 1 - 4.

[12] D. Betancourt et al., "Bending and folding effect study of the flexible, fully-printed and late-stage codified chipless RFID tags," *IEEE Transactions on Antennas and Propagation*, Vol. 64, No. 7, pp. 2815 – 2823, Jul. 2016.

[13] M. Barahona, D. Betancourt and F. Ellinger, "Comparison of UWB chipless RFID tags on flexible substrates fabricated using Aluminum, Copper or Silver," *IEEE-APS Topical Conference on Antennas and Propagation in Wireless Communications (IEEE-APWC)*, in press.

[14] A. Vena, E. Perret, and S. Tedjini, "High-capacity chipless RFID tag insensitive to the polarization," *IEEE Transactions on Antennas and Propagation*, Vol. 60, No. 10, pp. 4509 – 4515, Oct. 2012.

[15] W. Hays, *Statistics*, 5th Edition, Harcourt Brace College Publishers, Florida, 1994.

[16] J. Proakis, and D. Manolakis, *Digital Signal Processing*, 3rd Edition, Prentice-Hall, Inc., New Jersey, 1996.

[17] M. Barahona, D. Betancourt and F. Ellinger, "On the Decoding of Equiprobable UWB Chipless RFID Tags Using a Minimum Distance Detector," *International Symposium on Antennas and Propagation (ISAP)*, in press.